Spatially Anisotropic Etching of Graphite by Hyperthermal Atomic Oxygen†

Kenneth T. Nicholson,‡ Timothy K. Minton,*,§ and S. J. Sibener*,‡

The James Franck Institute and Department of Chemistry, The University of Chicago, 5640 South Ellis Avenue, Chicago, Illinois 60637, and Department of Chemistry and Biochemistry, 108 Gaines Hall, Montana State University, Bozeman, Montana 59717

Received: September 7, 2004; In Final Form: December 17, 2004

The spatially anisotropic kinetics involved in the chemical reaction between highly ordered pyrolytic graphite (HOPG) and a beam containing hyperthermal (∼8 km s^{-1}) $O(^3P)$ atomic oxygen and molecular oxygen yields unique surface morphologies. Upon exposure at moderate sample temperatures (298−423 K), numerous multilayer circular pits embedded in the reacted areas have been observed with the use of atomic force microscopy and scanning tunneling microscopy. These pits have diameters spanning nanometers to micrometers and depths from a few to tens of nanometers. The most striking characteristic of these pits is the convex curvature of the pit bottoms, where the highest point on the pit bottom is at the center and the lowest point occurs around the peripheral edge. Such structure arises by the interplay between kinetics of pit nucleation, the spatially anisotropic kinetics involved in the lateral and downward reactivity of HOPG, and the fluence of atomic oxygen. These kinetics, which are also influenced by the high reactivity of the translationally hot impinging oxygen atoms, govern the overall morphological evolution of the surface.

Introduction

The oxidation of carbon has been widely investigated because of its relevance to carbon combustion and water gas production,[1,2] removal of carbon deposits from catalysts,[3] and the durability of structural materials employed on spacecraft.[4−6] As a model system, the oxidation of highly ordered pyrolytic graphite (HOPG) has attracted particular interest. Molecular oxygen does not react with the basal plane of HOPG unless the sample temperature is >1500 K. O_2 reacts with prismatic carbon atoms to yield CO or CO_2, effectively removing one carbon atom from the surface, at sample temperatures >775 K.[8−10] As additional carbon atoms are removed around a defected site, monolayer and multilayer etch pits are created. However, the reaction probability is low, as these observations required the use of a high-temperature furnace and O_2 pressures of several Torr. Although HOPG has very low reactivity with molecular oxygen, both the basal and prism planes of HOPG are quite reactive to atomic oxygen even at moderate surface temperatures.[11−14] Surfaces exposed to oxygen atoms at thermal energies at room-temperature often contain hexagonal pits and other single and multilayer depressions. The O-atom generation method (microwave plasma, RF plasma, etc.) and the reaction conditions (fraction of atomic oxygen and overall pressure of reagent gas) have a strong effect on the morphology observed.

The surface morphology of HOPG exposed to hyperthermal (∼5 eV) oxygen atoms is qualitatively different from that seen when HOPG is exposed to thermal atomic oxygen. Studies in the hyperthermal energy range are important for reasons extending beyond fundamental surface science because they also model gas−surface collision events which occur in the low-Earth-orbit, $O(^3P)$ rich, chemical environment. Preliminary studies on the interaction between a beam containing hyperthermal atomic oxygen with HOPG have shown that the overall chemistry is marked by two distinctive characteristics, high reaction rate even at modest sample temperatures (298−493 K) and directionally specific O-atom reactivity that results in anisotropic etching in the downward interplanar and the intraplanar lateral directions. This anisotropy not only produces unique surface morphologies but is also surface temperature dependent. For example, at a sample temperature of 298 K, HOPG was etched at an overall rate commensurate with the removal of 1 C atom for every incident 22 O atoms, $\sim 3.0 \times 10^{-25}$ cm^3 per O atom assuming that the atomic oxygen component of the impinging hyperthermal beam dominated the reactivity.[4,5] The resulting surface morphology was rough on an atomic scale, while still decorated with numerous circular etch pits whose diameters span nanometers to microns and whose depths range from a few to tens of nanometers, depending on the O-atom fluence. When the sample temperature was increased to 493 K, the overall reaction probability increased to ∼1 C atom removed for every 8 incident O atoms. The resulting surface morphology was also considerably different, exhibiting no circular pits but instead large towers and hillocks spanning hundreds of nanometers. The increase in overall reaction rate was attributed to the greater number of prismatic carbon sites exposed in the hillock morphology.[4,5]

The purpose of this paper is to examine the anisotropic surface kinetics behind the growth of multilayer cylindrical pits in HOPG upon exposure to hyperthermal atomic oxygen at sample temperatures in the range 298−423 K. Beyond the nearly perfect cylindrical shape, the most striking characteristic of these pits is the convex curvature of their bottoms, with the highest point being near the pit center and the deepest point occurring around the peripheral edge of the bottom. In contrast to the rest of the reacted surface, the curved pit bottom exposes additional prismatic carbon sites, one for every single atom or multiatom step toward the center of the etch pit. Because prismatic atoms react at a faster rate than the atoms that make up the basal plane, the rate of reaction inside the cylinders is increased beyond the

† Part of the special issue "George W. Flynn Festschrift".

* To whom correspondence should be addressed. E-mails: (S.J.S.) s-sibener@uchicago.edu; (T.K.M.) tminton@montana.edu.

‡ The University of Chicago.

§ Montana State University.

10.1021/jp045960c CCC: $30.25
Published on Web 03/09/2005

reaction rate of the rest of the surface. These etch pits, which may have depths of tens of nanometers, therefore persist even after the overall surface has been etched several micrometers. The circular pits are continually deepened by the removal of graphite sheets laterally from the periphery to the center of the pit and widened by the removal of carbon at the prism plane presented at the periphery. These results illustrate the sensitive interplay between surface morphological change and the anisotropic reactivity of a hyperthermal atomic oxygen beam with HOPG.

Experimental Details

HOPG samples were exposed to a pulsed hyperthermal beam containing $O(^3P)$ atoms and molecular oxygen, with an $O:O_2$ ratio of approximately 0.70:0.30. The sample exposures and beam characterization methods were conducted in a manner similar to those described in ref 15. Other characteristics of the hyperthermal source and the apparatus may be found in refs 16−18. In short, the molecular beam source is based on the laser detonation source originally developed by Physical Sciences, Inc.[19] All samples were exposed at a distance of 40 cm from the source, and a Kapton H reference sample accompanied each exposure. The etch depth of this reference sample was used to determine a "Kapton-equivalent O-atom fluence" of the beam.[15] The pulsed source operated at a repetition rate of 2 Hz, and the estimated O-atom fluence per pulse at the sample surfaces was 1.75×10^{15} O atoms cm^{-2}. The nominal beam velocity was 8000 m s^{-1}, and the velocity spread was ∼2400 m s^{-1} (full width at half-maximum).

Before mounting in the vacuum chamber, the HOPG samples were cleaved several times with the use of Scotch tape. Atomically resolved scanning tunneling microscopy (STM) images confirmed that the cleaved surfaces yielded several large terraces that did not contain any defects. The samples, approximately 1 × 1 cm, were placed in a sample mount whose temperature can be controlled from 298 to 573 K. A square mesh of stainless steel was placed over the samples during the exposures in order to facilitate measurements of overall etch depth. Open squares within the mask exposed several hundred square micrometers in area to the atomic oxygen beam. A DEKTAK3 surface profiler was used to measure the depth of graphite removed in the squares with respect to the covered areas. This, in turn, allowed direct determination of the overall etching probability, in terms of the number of C atoms removed per incident O atom. This overall etching probability is not site specific but rather represents an integrated metric for reactivity. The hyperthermal impact of molecular oxygen may also play a role in the formation of products. Therefore, the O-atom fluence used to derive the etching probability is an effective fluence which may include collisional effects due to the molecular oxygen in the beam.

The surface morphology of HOPG was imaged at room temperature with the use of a Topometrix Discoverer AFM/STM system. All the images contained in this paper were leveled using a three-point reference. Line scans, surface roughness measurements, and all other image analyses utilized Topometrix software. For determining the reaction probability of the prism C sites, the average diameter of the largest 10% of the cylinders found on each sample was used. All pits were assumed to nucleate at their centers at $t = 0$ and expand outward as a function of time. This assumption is valid because it has been experimentally observed that the diameter of the largest 10% of the cylinders increased linearly with exposure time.[5] The distance from the center of the pit to the peripheral edge provided a known number of carbon atoms removed, given the unit cell for HOPG.

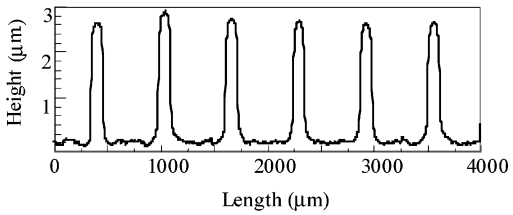

Figure 1. Surface profile of HOPG that was etched with a stainless steel mesh covering the surface. The step height difference between protected and unprotected areas of the sample provides a measure of the etch depth.

Results and Discussion

Figure 1 highlights the macroscopic erosion of HOPG by illustrating the observed height difference between protected and unprotected areas of the HOPG sample. According to these profilometric measurements, ∼2.7 μm of graphite (nearly 9000 sheets) are completely removed after exposure to $\sim 3.5 \times 10^{20}$ O atoms cm^{-2} at a sample temperature of 373 K. This corresponds to an overall reaction probability, $P_{overall}$, of 0.083 or, in other terms, 1 C atom removed for every 12 incident hyperthermal $O(^3P)$ atoms.

The early stages in the formation of circular pits have been probed by imaging the HOPG surface after exposure to a low fluence of atomic oxygen. A representative STM image (100 × 100 nm), taken after the graphite sample at 373 K had been exposed to 5×10^{17} O atoms cm^{-2}, is shown in Figure 2A. The first notable characteristic is the presence of multiatomic carbon vacancies on the surface. A few pitlike features are also observed which have diameters and depths on the nanometer scale; however, a clear hexagonal or circular shape is not discernible. Thus, even after the sample has reacted with only ∼100 monolayers of $O(^3P)$, no pristine areas of graphite (on the order of several nanometers) remain. It has also been determined that the root-mean-square (RMS) surface roughness also increases with O-atom exposure. These observations may be viewed as an extension of what has been reported in a study of graphite erosion by low fluences of hyperthermal atomic oxygen.[6] Unlike this current study which describes the morphologies observed after an exposure range of 5×10^{17} to 3.1×10^{20} O atoms cm^{-2}, the referenced work discussed exposures ranging from 10^{15} to 10^{17} O atoms cm^{-2} and the formation of point defects upon sub-monolayer fluences of O atoms. The surface was further roughened with increasing atomic oxygen fluence where small pits surrounded by "hillocks" were imaged. Figure 2A is qualitatively consistent with that reported in the referenced work.

The etched areas of HOPG surfaces exposed to greater than 5.0×10^{18} atoms cm^{-2} of hyperthermal atomic oxygen contain numerous circular pits of various diameter and depth. Atomic force microscopy (AFM) images of representative pits observed for two different O-atom fluences are illustrated in Figure 2B,C. The mean diameter of the widest 10% of the pits increases linearly with hyperthermal atomic oxygen exposure.[5] Therefore, the largest etch pits must have nucleated at or near the topmost graphite layer; otherwise the same distribution of diameters would be observed regardless of O-atom fluence. Smaller pits, on the order of tens of nanometers in diameter, have been observed after every exposure. These smaller pits are also frequently embedded in the bottoms of the larger pits, Figure 2D.

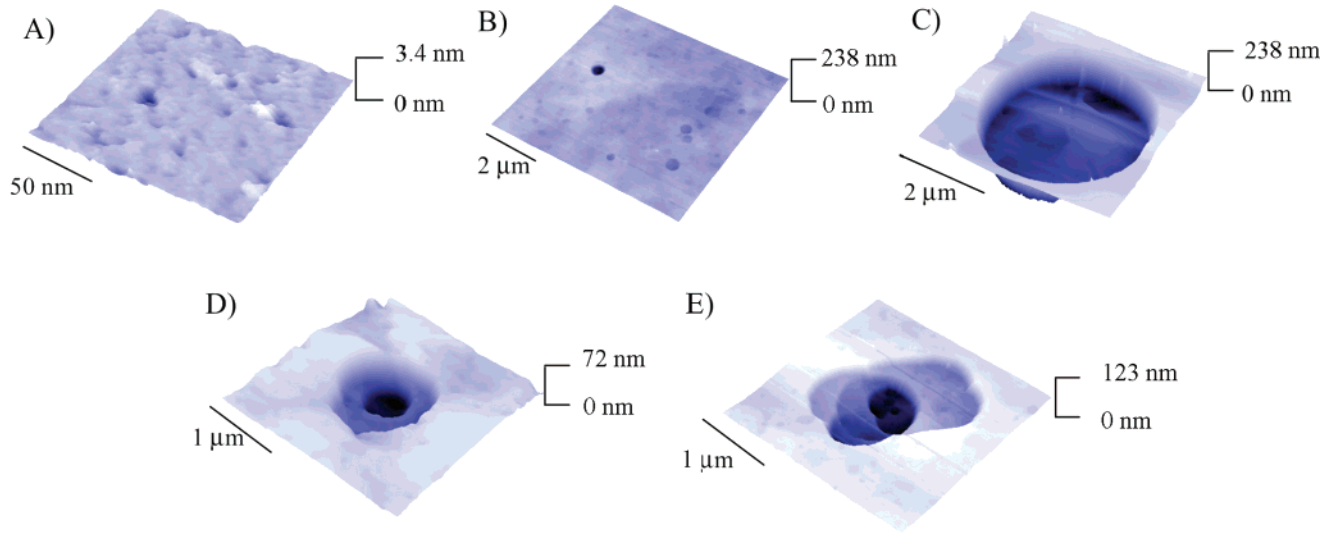

Figure 2. (A) STM image (100 nm × 100 nm) of HOPG after exposure to 5×10^{17} O atoms cm^{-2} at near normal incidence. (B) AFM image (15 μm × 15 μm) of HOPG after exposure to 9.4×10^{19} O atoms cm^{-2}. (C) AFM image (8.8 μm × 8.8 μm) of a representative circular pit observed in a sample that was exposed to 3.6×10^{20} atoms cm^{-2}. (D) AFM image (5 μm × 5 μm) of a small pit growing inside of a large circular cavity. (E) AFM image (5 μm × 5 μm) of a pit merging event. The sample temperature during these exposures was 373 K.

A statistical analysis of the diameters of the largest pits provides a direct measure of P_{prism}. Prismatic carbon atoms refer to atoms surrounding a point or extended defect site. Any intraplanar reactivity of a carbon atom is termed herein as reaction in the prism plane. Chemistry in the downward or interplanar direction, where the reacted carbon atoms are sp^2 hybridized, is described as reaction in the basal plane. Figure 3A illustrates a plot for HOPG etching at 373 K in which the average diameter of the widest 10% of the pits is represented as the number of edge carbon atoms, and this quantity is plotted as a function of exposure time. Using the average O-atom flux of 3.5×10^{15} atoms cm^{-2} s^{-1}, a value for P_{prism} of 0.44 or roughly 1 C atom for every 2.3 incident O atoms has been derived. Increasing the sample temperature leads to pits with larger diameters after the same O-atom exposure fluence. This observation suggests that P_{prism} is dependent on the surface temperature, even though the incident O atoms have translational energies of ~5 eV. Treated effectively as a zero-order reaction due to the linear relationship between pit diameter and O atom exposure, a rate constant has been derived. Since the average diameter of the largest 10% of the circular pits is being considered for this calculation, all of the pits have been assumed to nucleate at the top layer of the HOPG, with $t_0 = 0$. The calculated rate constant, k_{prism}, is 2.43×10^{-1} s^{-1} at 373 K. This rate constant appears to have an Arrhenius temperature dependence, with an activation energy, E_a (for the temperature range 298−423 K), of 10.5 kJ/mol, Figure 3B. This activation energy is lower than that calculated for molecular and thermal atomic oxygen reactivity with HOPG, suggesting that the high translational energy of the impinging O atoms has a role in traversing the reaction coordinate.[9,10,12] The Arrhenius behavior of the rate constant also suggests a process which is dependent upon surface temperature and is also involved in the formation of products, presumably CO and CO_2. The diameter of the circular pits expands according to k_{prism} from the point of nucleation until another pit of similar depth is encountered. Numerous pit merging events have been observed, and appear to be most common for the smaller, shallower pits (Figure 2E).

The final depths of the pits and the morphology of the pit bottoms are governed by the nature of the nucleation event, O-atom fluence, and anistropic reaction kinetics, even when a beam containing hyperthermal atomic oxygen is employed. The nature of the nucleation event is expected to have a role because deepening could first occur along a defect site or grain boundary (because P_{prism} is larger than P_{basal}), presumably until a pristine graphite sheet is encountered. This deepening would also be much faster than the erosion of the rest of the surface, $P_{overall}$,

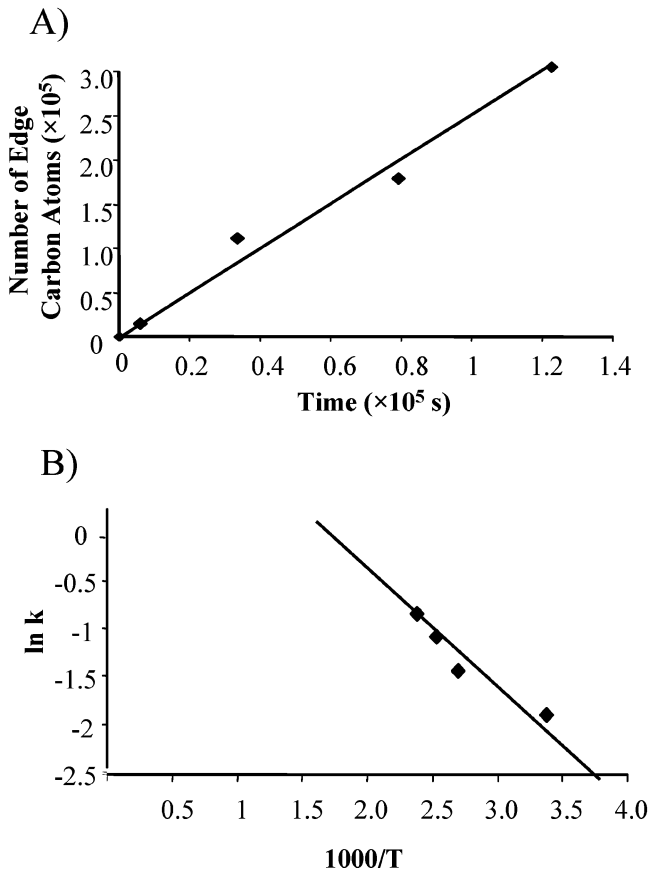

Figure 3. (A) Plot of the average diameter of the widest 10% of the pits, represented in the number nearest neighbor carbon atoms (nearest neighbor spacing = 0.24 nm), as a function of exposure time, for a sample temperature of 373 K. The slope of the line that fits the data is taken to be the zero-order rate constant, k_{prism}. (B) Arrhenius plot for k_{prism} in the temperature range 298−423 K. The activation energy derived is $E_a = 10.5$ kJ/mol.

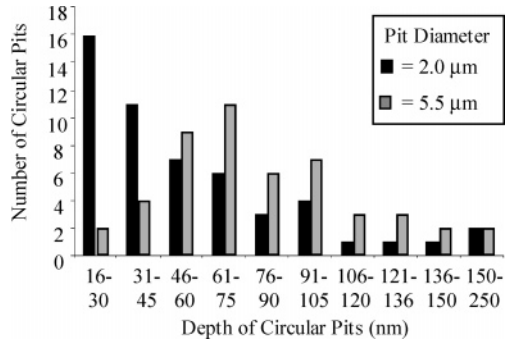

Figure 4. Histogram of pit depths. Diameters of 2.0 ± 0.1 μm (black) and 5.5 ± 0.1 μm (shaded) were chosen to illustrate the broad distribution of pit depths and the increase in depth with increasing diameter.

or a pit would not be observed. A large, multilayer pit, may also nucleate from the merging of two or more pits during the erosion process.

The nucleation event does not ultimately determine the final depth of the pit because the pits become, on average, deeper as they widen, Figure 4. There is a broad distribution of pit depths for pits of constant diameter and therefore constant O-atom fluence after the initial nucleation event, Figure 3. The distribution of pit depths with diameter of 2 μm is much shallower than those with diameter of 5.5 μm, illustrating the role of O-atom fluence on pit depth. However, unlike the diameter, pit deepening is not linear with O atom exposure. Furthermore, the pits become deeper, on average, as they widen, indicating that the pits are deepening faster than the remainder of the etched surface which is also being exposed to the hyperthermal atomic oxygen beam. As mentioned above, the remainder of the surface is rough (RMS roughness = 16 nm for samples exposed at 373 K) with numerous basal and prism carbon atoms exposed. The pit bottoms have a *curved* morphology, convex with the highest point near the center and deepest points around the peripheral edge.

The curved morphology, combined with the anisotropic reaction kinetics, deepens the pits at a faster rate than the rest of the HOPG surface that is exposed to the hyperthermal atomic oxygen. A three-dimensional representation of a pit with a diameter of 6.1 μm (at the top layer) and a depth of 152 nm is illustrated in Figure 5. This cavity is one of the widest imaged for this particular sample (T_{sample} = 373 K) during an exposure of 3.6 × 10^{20} O atoms cm^{-2}. The curvature suggests that the carbon atoms near the periphery have a higher reaction probability with the impinging hyperthermal atomic oxygen than the other carbon atoms inside the pit. This enhanced reaction probability may be correlated to an electronic effect, where the carbon atoms at and near the peripheral edges of deep cylindrical pits are more reactive than those in the center. A more likely explanation is that grazing-angle scattering of O atoms from the emerging pit sidewall leads to a relatively high flux of energetic O atoms around the peripheral edge of the pit, thus enhancing the rate of carbon atom removal in this localized region. Similar trenching at the base of a sidewall has been observed earlier in the etching of silicon by a beam of hyperthermal fluorine atoms, and this phenomenon was explained by the concentration of energetic fluorine atoms following inelastic scattering from the sidewall.[21] This sidewall scattering in graphite could also lead to step bunching, a situation where several atomic steps are in very close proximity to one another. The instability of step bunches has been reported, often leading to higher reaction rates in those localized regions.[22] This

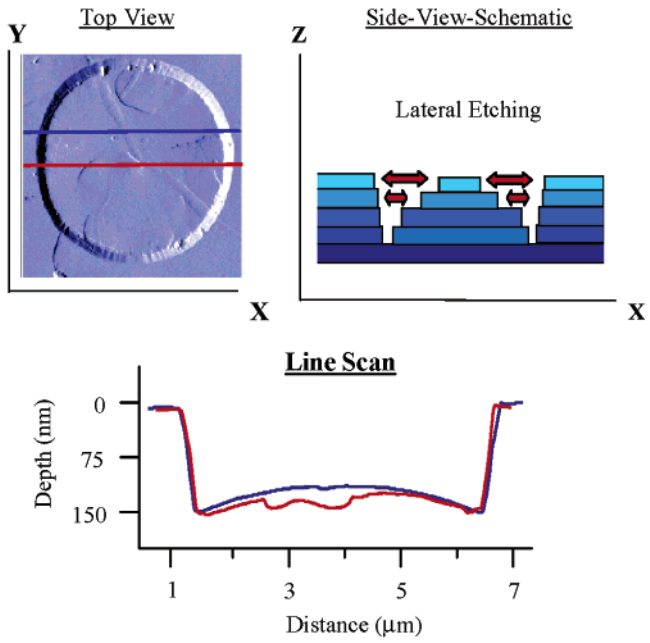

Figure 5. (A) AFM image (shading used to highlight depth morphology) of a large circular pit found in an HOPG surface after exposure to 3.6 × 10^{20} O atoms cm^{-2} near normal incidence. The sample temperature during the exposure was 373 K. (B) Line scans that illustrate the shape of the bottom of this pit.

would further facilitate the downward etching process near the peripheral edge of the large circular pits. As the peripheral edge becomes deeper, the rate of the overall cylinder deepening continually increases as more prism carbon atoms become exposed. The exposure of these prism or edge carbon atoms along the convex pit bottom facilitates the deepening of the pits by lateral reactivity, with probability, P_{prism}. The actual curvature quantifies the relative rates involved in the governing anisotropic kinetics of graphite reactivity with hyperthermal atomic oxygen.

The height difference between the center of a pit and the peripheral edge of its bottom provides a simple measure of the curvature. This height difference can be equated, through the dimensions of the unit cell, with a number of graphite layers. Only pits with significant diameter (>400 nm) and depth (>20 nm) had measurable curvature. To characterize the curvature of a pit, line scans were taken from three directions, all crossing at the center of the pit. Often, the pit bottom was found to be asymmetric—i.e., the measured height difference varied for each line scan. This asymmetry results from the slightly off-normal incidence of the beam at the sample due to the geometry of the sample mount. In all cases, the average height from the line scans was taken to represent the curvature of a pit bottom.

Figure 6 shows plots of the height difference (or pit curvature) in the number of carbon layers versus the pit radius represented as the number of carbon atoms from the pit center to the outside edge. Lines corresponding to three different sample temperatures are shown. At T_{sample} = 373 K, the average lateral distance traveled before an atomic step is encountered (revealing the next HOPG sheet) is 176 carbon atoms, or ~65 nm. When the sample temperature is increased, the curvature is magnified. At T_{sample} = 423 K, one atomic step is encountered for every 100 lateral C atoms. Therefore, at higher temperatures, the curvature is enhanced, presumably because the downward etch rate at the periphery of a pit increases faster than the lateral etch rate.

Summary

The etching of HOPG by a beam of hyperthermal atomic oxygen at moderate sample temperatures yields a unique surface

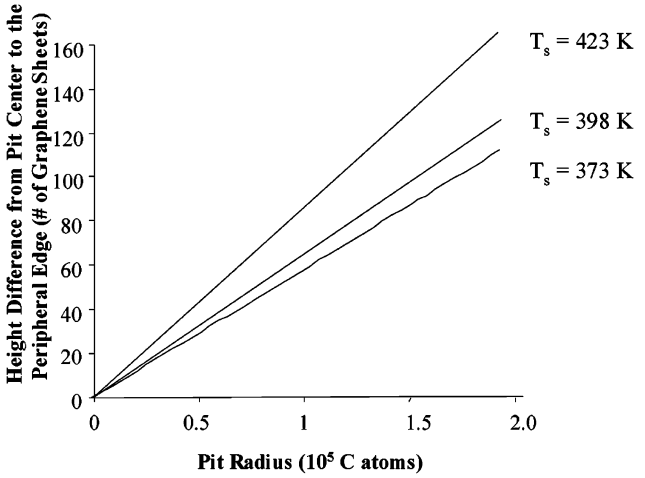

Figure 6. Plot illustrating the curvature of pit bottoms formed when HOPG samples at temperatures of 373, 398, and 423 K were exposed to the hyperthermal O-atom beam at a fluence of 3.6×10^{20} O atoms cm^{-2}. These data represent the height difference, in the number of graphite sheets (HOPG sheet spacing = 0.34 nm) between the center of the cylinder and the peripheral edge as a function of the radius of the pit.

morphology consisting of an atomically rough surface with numerous embedded multilayer circular pits. These pits nucleate at different times during the etching process at newly formed or preexisting defect sites and, from that point, grow deeper and wider. The pits have shallow aspect ratios and diameters may be hundreds of nanometers to a few micrometers, while depths reach only tens of nanometers. Despite these relatively shallow depths, the pits persist even after several micrometers of the HOPG surface have been etched by the beam. This observation and a detailed investigation of the growth kinetics of the craters both laterally and in depth suggest that anisotropic reactivity both creates the pits and yields an etch rate inside the pit that is higher than the overall etch rate of the HOPG surface in the temperature range, 298−423 K. The lateral growth as measured by the diameter of the pit increases linearly as a function of O-atom fluence. The initial pit nucleation event, total O-atom fluence, and the anisotropic etch kinetics within the pits each appear to influence the final pit depth.

The pits are deeper around the periphery than in the center and thus exhibit curved (convex) bottoms. The curvature is direct evidence of a higher reaction probability for C atoms near the periphery of the deep circular pits in comparison to C atoms that are away from the periphery. This is likely due to an electronic effect and/or higher effective O-atom fluence at the peripheral edge due to scattering at the pit walls. The creation of step bunches with their associated heightened reactivity during O atom exposure may further enhance the rate of pit deepening at the periphery. The curvature itself results from sequential layer-by-layer reactivity inward from the periphery, with the rate of lateral intraplanar reaction being faster than that characteristic of downward interplanar reactivity. Differential changes in these spatially anisotropic reaction rates as a function of substrate temperature are illustrated by commensurate changes in pit curvature. Such temperature-dependent kinetics can in fact lead to dramatic changes in overall surface morphology, as shown in ref 4.

The results presented in this paper demonstrate that the kinetics and dynamics of hyperthermal atomic oxygen erosion of graphite differ markedly from those typically seen for thermal atomic and molecular oxygen. This is evidenced not only by changes in the overall reactivity but especially by the observed morphological presentation of the etched interface. These studies have important implications for both combustion processes and the stability of high-performance materials in chemical environments which contain hyperthermal reagents.

Acknowledgment. These experiments were primarily supported by the AFOSR sponsored MURI Center for Materials Chemistry in the Space Environment. Supplemental support from The University of Chicago—Argonne National Laboratory Consortium for Nanoscience Research and the National Science Foundation—Materials Research Science and Engineering Center at The University of Chicago are also gratefully acknowledged. Jalice Manso is thanked for her assistance in the profilometry measurements and in the atomic oxygen exposures. Amadou Cisse and Devon Pennington are thanked for their contributions in sample imaging.

References and Notes

(1) Chang, H.; Bard, A. J. *J. Am. Chem. Soc*. **1991**, *113*, 5588.

(2) Phillip, J.; Polwart, N.; Troupe, C. E.; Wilson, J. I. B. *J. Am. Chem. Soc*. **2003**, *125*, 6600.

(3) Yang, Y. W.; Hrbek, J. *J. Phys. Chem. B* **1995**, *99*, 3229.

(4) Nicholson, K. T.; Minton, T. K.; Sibener, S. J. *Prog. Org. Coat.* **2003**, *47*, 443.

(5) Nicholson, K. T.; Minton, T. K.; Sibener, S. J. *Proceedings for the 9th International Symposium for Materials in the Space Environment*, Noordwijk, The Netherlands, June 16−20, 2003 (ESA SP-540, September 2003); European Space Agency: Noordwijk, The Netherlands, 2003; pp 481−485.

(6) Kinoshita, H.; Umeno, M.; Tagawa, O. *Surf. Sci.* **1999**, *440*, 49.

(7) Olander, D. R.; Siekhous, W.; Jones, R.; Schwarz, J. A. *J. Chem. Phys.* **1972**, *57*, 408.

(8) Olander, D. R.; R. H.; Schwarz, J. A.; Siekhaus, W. J. *J. Chem. Phys.* **1972**, *57*, 421.

(9) Stevens, F.; Kolodny, L. A.; Beebe, T. P. *J. Phys. Chem. B* **1998**, *102*, 10799.

(10) Lee, S. M.; Lee, Y. H.; Hwang, Y. G.; Hahn, J. R.; Kang, H. *Phys. Rev. Lett.* **1999**, *82*, 217.

(11) Wong, C.; Yang, R. T.; Halpern, R. T. *J. Chem. Phys*. **1983**, *78*, 3325.

(12) Paredes, J. I.; Martinez-Alonso, A.; Tascon, J. M. D. *Langmuir* **2002**, *18*, 4214, and references therein.

(13) You, H.-X.; Brown, N. M. D.; Al-Assadi, K. F. *Surf. Sci*. **1993**, *284*, 263.

(14) Incze, A.; Pasturel, A.; Chatillon, C. *Surf. Sci.* **2003**, *537*, 55.

(15) Brunsvold, A. L.; Minton, T. K.; Gouzman, I.; Grossman, E.; Gonzalez, R. I. *High Perform. Polym*. **2004**, *16*, 303.

(16) Minton, T. K.; Garton, D. J. Dynamics of Atomic-Oxygen-Induced Polymer Degradation in Low Earth Orbit. In *Advanced Series in Physical Chemistry: Chemical Dynamics in Extreme Environments*; Dressler, R. A., Ed.; World Scientific: Singapore, 2001; pp 420−489.

(17) Zhang, J.; Garton, D. J.; Minton, T. K. *J. Chem. Phys.* **2002**, *117*, 6239.

(18) Garton, D. J.; Minton, T. K.; Maiti, B.; Troya, D.; Schatz, G. C. *J. Chem. Phys.* **2003**, *118*, 1585.

(19) Caledonia, G. E.; Krech, R. H.; Green, D. B. *AIAA J*. **1987**, *25*, 59.

(20) Zhang, J.; Minton, T. K. *High Perform. Polym*. **2001**, *13*, S467.

(21) Hwang, G. S.; Anderson, C. M.; Gordon, M. J.; Moore, T. A.; Minton, T. K.; Giapis, K. P. *Phys. Rev. Lett.* **1998**, *77*, 3049.

(22) Sangwal, K.; Clemente, R. R. *Surface Morphology of Crystalline Materials*; Sci-Tech Publications: Vaduz, Liechtenstein, 1991.